

PDF hosted at the Radboud Repository of the Radboud University Nijmegen

The following full text is a publisher's version.

For additional information about this publication click this link.

<http://hdl.handle.net/2066/98822>

Please be advised that this information was generated on 2021-04-11 and may be subject to change.

The far-infrared spectra of neutral and cationic niobium clusters: $\text{Nb}_5^{0/+}$ to $\text{Nb}_9^{0/+}$

André Fielicke^{a)}

Fritz-Haber-Institut der Max-Planck-Gesellschaft, Faradayweg 4-6, D-14195 Berlin, Germany

Christian Ratsch^{b)}

Fritz-Haber-Institut der Max-Planck-Gesellschaft, Faradayweg 4-6, D-14195 Berlin, Germany, Department of Mathematics, UCLA, Los Angeles, California 90095-1555, USA, and California NanoSystems Institute, UCLA, Los Angeles, California 90095-1555, USA

Gert von Helden and Gerard Meijer

Fritz-Haber-Institut der Max-Planck-Gesellschaft, Faradayweg 4-6, D-14195 Berlin, Germany

(Received 29 August 2007; accepted 12 October 2007; published online 18 December 2007)

Far-infrared absorption spectra of small neutral and cationic niobium clusters containing five to nine Nb atoms have been obtained by multiple photon dissociation spectroscopy of their argon complexes. The experimental far-IR spectra are recorded in the 85–600 cm^{-1} region and cover the range of the structure-specific vibrational fundamentals, i.e., the finger-print range, for these metal clusters. The experiments are accompanied by quantum chemical calculations employing the density-functional theory. A comparison of the experimental and calculated far-IR spectra allows to identify the cluster structures. Although the experimental spectra for clusters containing five, six, eight, and nine Nb atoms are very different for cationic and neutral clusters, the comparison with theory reveals that, nevertheless, the overall geometries for cations and neutrals are very similar, except for $\text{Nb}_6^{0/+}$. © 2007 American Institute of Physics. [DOI: 10.1063/1.2806176]

I. INTRODUCTION

Small particles often differ considerably in their properties from the bulk material. This has triggered a large interest in the study of matter on the nanoscale, but the basic determination of the structure of nanomaterials on an atomic scale can be exceedingly difficult.¹ Even when the atomic composition is known, as for isolated gas-phase nanoparticles or clusters, the determination of their geometric structures is still very challenging. However, knowing the atomic arrangements of gas-phase clusters is one of the crucial ingredients that is needed for understanding their physical and chemical properties.

Recently, new experimental techniques that are sensitive to the geometric structure have been applied to gas-phase metal clusters, such as measurements of ion mobilities,^{2,3} electron diffraction on trapped cluster ions,^{4,5} or high resolution anion photoelectron spectroscopy.^{6,7} Particularly sensitive to the internal cluster structure is vibrational spectroscopy, since it directly maps the bonding forces and, in its appropriate variant, it is susceptible to the cluster symmetry.⁸ We have recently demonstrated far-infrared multiple photon dissociation (far-IR-MPD) spectroscopy on transition metal cluster rare-gas complexes as a method to obtain the vibrational spectra in the range of their structure-specific vibrational fundamentals.⁹ Far-IR spectra of vanadium clusters containing between 3 and 23 atoms have been reported. A comparison of calculated vibrational spectra for different

cluster geometries obtained using the density-functional theory (DFT) with those obtained in the experiment allows to deduce the cluster-size specific structures. Using this approach for the vanadium clusters, for several cluster sizes the atomic structures have been clearly identified.^{9,10} It has been shown that in most cases the rare-gas atom does not significantly influence the vibrational spectrum and merely acts as a probe for detecting the resonant absorption of IR photons by the metal cluster.^{10,11}

We have now applied this technique to small neutral and cationic niobium clusters. Partly because of their relative ease of production and the favorable isotopic distribution, niobium clusters have been intensively investigated experimentally and this has been followed by extensive theoretical studies. Experimental studies include single and multiphoton ionizations,^{13–16} as well as photoelectron spectroscopy^{17–20} and the measurements of the bond dissociation energies.^{21,22} Optical absorption spectra of neutral niobium clusters have been measured by means of photodissociation of their complexes with rare-gas atoms^{23–25} and this technique is also used here for obtaining the vibrational spectra.

Niobium clusters show interesting size effects in their gas phase reactivity, e.g., towards hydrogen, nitrogen, or small hydrocarbons.^{13,26–35} The reaction rate towards H_2 and N_2 is found to correlate with the electronic properties as expressed, e.g., by an (effective) ionization potential of the cluster.^{13,34} The presence of isomers for several cationic and neutral clusters in the size range between 9–20 atoms has been observed in reactivity studies^{30–35} but also spectroscopically.^{12,14,15} In electric deflection experiments on neutral niobium clusters a strong variation in the per-atom

^{a)}Electronic mail: fielicke@fhi-berlin.mpg.de

^{b)}Electronic mail: cratsch@math.ucla.edu

polarizability has been found and it has been suggested that this is related to large size-dependent variations in the electronic or geometric structures.³⁶ At cryogenic temperature neutral niobium clusters show a permanent electric dipole moment implying that they are ferroelectric, but that vanishes at higher temperature or upon laser heating.^{37,38} This behavior is explained by a two component model that assumes a low-energy transition between two electronically very different states of the cluster, but the nature of these states is not understood.

First-principles electronic structure calculations have been applied in numerous studies to investigate electronic and geometric structures of niobium clusters. Mainly the density-functional theory has been employed to study their geometric and electronic structures with the aim to find correlations with experimental observations, e.g., on the size dependence of reactivities, electron binding energies, or bond dissociation energies.^{17,39–50} The multireference character of the wavefunctions of small niobium clusters containing three to five atoms has been taken into account by using the complete active space multiconfiguration self-consistent field method followed by the multireference singles plus doubles configuration interaction.^{43–45} This approach generally gives similar ground state structures compared to DFT, although it is expected that explicit treatment of the interaction of different electronic configurations leads to a better description of the various low-lying electronic states. The identification of global minima becomes more complicated for larger clusters where the success of the traditional gradient following techniques strongly depends on the accurate choice of the starting structures. The application of global search algorithms solves this problem and such methods have recently been applied for structure optimization of niobium clusters.^{51–54}

Although, in principle, these techniques are able to identify the lowest energy structure within the applied theoretical model, those structures can be different to the ones present in the experiments. This can be due to the limits of the theoretical approach, or because in the experiments the cluster growth mechanism might favor isomers of higher energy that are kinetically stabilized. To check for these effects, experimental probes of the cluster structures are required as provided, for instance, by the vibrational spectrum. In case of niobium clusters, the neutral dimer and trimer have been investigated before in the gas phase and embedded in rare-gas matrices. Using the matrix isolation resonance Raman spectroscopy the dimer stretching frequency was found to be $\omega_e = 421 \text{ cm}^{-1}$,^{55,56} in agreement with the gas-phase value of 424.9 cm^{-1} from the rotationally resolved electronic spectrum.⁵⁷ For the trimer, vibrational fundamentals of 235 and 227 cm^{-1} have been derived from the observed band progressions in the Raman spectrum and they are assigned to the totally symmetric stretch and the doubly degenerate bend of a nearly D_{3h} symmetric structure.⁵⁸ Theory identifies a triangular 2B_1 state with an obtuse angle of 63.4° as the ground state for this species.⁴⁵

In our study we focus on slightly larger niobium clusters containing five to nine atoms. The lower limit of this range is determined by experimental constraints; for smaller clusters

the abundance of the rare-gas complexes in the beam becomes too low. For clusters with more than nine atoms, we suppose a more evolved theoretical approach for probing the configurational space would be needed. In the following we present the experimental far-infrared vibrational spectra of cationic and neutral niobium clusters and compare them with calculated spectra obtained for energetically low-lying isomers.

II. EXPERIMENTAL

The experiments are performed in a molecular beam machine that is permanently coupled to a beam line of the “Free Electron Laser for Infrared eXperiments⁵⁹” (FELIX) located at the FOM Institute for Plasma Physics in Nieuwegein, The Netherlands. This setup and the experimental procedure to record IR spectra have been described in detail before.¹¹

In short, neutral and charged metal clusters are produced by pulsed laser ablation in a source that is in part cooled to 80 K. At this temperature the metal clusters can form complexes with Ar that is admixed to the He carrier gas. The Ar concentration is typically 20% to form complexes with the neutral clusters and only 0.5% for the cations. After leaving the source, the cluster beam is shaped by a skimmer and an aperture with 1 mm diameter opening before it enters the extraction range of a reflectron time-of-flight mass spectrometer. Neutral clusters are ionized with 6.42 eV photons from an ArF excimer laser.

Before detection in the mass spectrometer the cluster beam is irradiated with the counterpropagating IR beam, which is loosely focused on the aperture. The absorption of multiple IR photons by a cluster complex can lead to its fragmentation and the resulting reduction of the abundance of the Ar complex is size-selectively measured as a function of the IR wavelength. From these “depletion spectra,” absorption spectra are constructed, taking the intensity changes of the IR radiation over the scanning range into account. Details of the conversion procedure are reported elsewhere.¹¹ In general, an absorption of multiple far-IR photons is required to overcome the barrier for dissociation of the Ar complex within the time window of $\approx 40 \mu\text{s}$ between IR irradiation and arrival in the time-of-flight mass spectrometer.

For the experiments on the niobium clusters FELIX is tuned between 85 and 600 cm^{-1} . In this range a single IR macropulse contains an energy of 10–40 mJ at a macropulse length of 7–9 μs . The bandwidth of the emitted far-IR radiation is adjusted to be about 1% of the central frequency (full width at half maximum). The central frequency has been calibrated with a grating spectrometer resulting in an absolute accuracy of better than 0.5 cm^{-1} for the reported experimental spectra. These spectra are composed of averages of 4–10 individual frequency scans, which amounts to an average of up to ≈ 500 single mass spectra per point.

III. THEORETICAL METHODS

We have performed DFT calculations to find the energetically most preferred structures for small neutral and cationic niobium clusters. The calculations were carried out us-

ing the DMOL³ code,⁶⁰ an all-electron code that uses numerical atomic orbitals as a basis set. It is an extremely efficient code for small clusters. The convergence of our basis set has been tested carefully, and for all the results reported below, a basis set is used that is labeled “all” in the code. This basis set includes the $1s$, $2s$, $2p$, $3s$, $3p$, $3d$, $4s$, $4p$, $4d$, $5s$, and $5p$ orbitals. The cutoff radius was 12 bohrs and the mesh parameter is 1.6. We used the generalized gradient approximation (GGA) for the exchange-correlation functional.⁶¹ These are essentially the same parameters and exchange-correlation functional as we used for our work on vanadium, where details of the convergence tests have been published in Ref. 10.

We calculated the ground state energy for a number of possible geometries for each cluster size. The initial geometries in the optimizations are the ones that have been previously discussed in the literature.^{39–44} Often these geometries are very similar to the ones of the corresponding vanadium clusters and, therefore, we tested, in particular, all the structures that have also been considered by us in our previous work on vanadium.¹⁰ In all calculations the atomic positions were completely relaxed. There were no symmetry constraints in the geometry optimization procedure. We also tested the different possible spin states for all clusters (see discussion below). The vibrational spectrum for each cluster has been calculated by displacing each atom in each direction, in order to evaluate the $3n$ dimensional force-constant matrix. No frequency scaling has been applied. The IR intensities have been obtained from the derivative of the dipole moment. All reported relative energies include the vibrational zero-point energies.

We note that our approach does not amount to a complete scan of the configuration space, and that, in particular, for larger clusters a more sophisticated approach to search for the ground state geometry is needed. But we suppose that for the cluster sizes discussed in this paper all relevant structures have been considered. This assessment is supported by the good agreement between the calculated and experimentally obtained vibrational spectra.

IV. RESULTS AND DISCUSSION

A. General remarks

Far-IR multiple photon dissociation spectra are obtained for the Ar complexes of the neutral and cationic niobium clusters in the $85\text{--}600\text{ cm}^{-1}$ range. The experimental spectra shown in Figs. 2–6 have been measured for the complexes with a single Ar atom, and no significant changes in the spectra have been observed for the complexes containing up to four Ar atoms, with the exception of Nb₉ (see below). Possible distortions in the far-IR-MPD spectra of a metal cluster Ar complex $M_n\text{Ar}_m$ arising from sequential Ar atom loss of $M_n\text{Ar}_{m+1}$ have been extensively discussed elsewhere.¹¹ Complexes with larger m show often more intense absorption bands and this effect becomes more pronounced with decreasing photon energy. In most cases, however, this affects the relative intensities of the observed bands only moderately. The frequencies of the absorption bands are hardly influenced by the Ar coverage. This small influence of

the Ar coverage on the observed far-IR-MPD indicates that the structure of the bare metal cluster is not significantly altered by the Ar binding. This conclusion is additionally supported by the results of the DFT calculations on the bare metal clusters, see below.

For clusters containing five to nine Nb atoms pronounced absorption bands are found in the $120\text{--}300\text{ cm}^{-1}$ range, and there are no bands observed above 300 cm^{-1} . This observation is in line with, both, the measured vibrational frequencies for the dimer and trimer species, and the frequencies of the bulk phonon modes for body centered cubic (bcc) niobium; the latter are found at $\approx 192\text{ cm}^{-1}$ (longitudinal modes) and at $\approx 129\text{ cm}^{-1}$ (transverse modes).^{63,64}

Calculated vibrational spectra for selected low-lying isomers are shown together with their structures above the experimental spectra in Figs. 2–6. The labels of the isomers indicate the number n of atoms in the cluster, the charge state, and the isomer (A, B, and C). The capital letter is chosen according to the ascending relative energies with A indicating the energetic minimum. For all isomers the vibrational fundamentals are found below 350 cm^{-1} , which gives us additional evidence that the experiment completely covers the higher energy part of the cluster vibrational spectra. Most bands are slightly blueshifted in the calculations with respect to their experimental counterparts, probably mainly due to the use of the harmonic approximation in the calculation of the vibrations. In addition, the experimental frequencies might have a general redshift due to the nature of the IR-MPD process.⁶² The calculated IR intensities are relatively low, on the order of up to 10 km mol^{-1} only.

Generally, the cationic and neutral niobium clusters are found to be more stable in the lowest possible electronic spin state. The only exception is Nb₅⁺, where the ground state is found to be a triplet in agreement with theoretical predictions. The low spin multiplicities correspond to the results of Stern-Gerlach-type experiments on the neutral niobium cluster that find magnetic moments of $0\ \mu_B$ for even-numbered clusters and close to $1\ \mu_B$ for most odd-numbered clusters.⁶⁵ As an additional check for consistency of our calculations we compare in Fig. 1 the calculated dissociation energies $D_{\text{Nb}_n}^0 = E_{\text{Nb}} + E_{\text{Nb}_{n-1}} - E_{\text{Nb}_n}$ and the ionization potentials for the finally assigned structures of the neutral niobium clusters with experimental values from the literature. Although the calculated values are slightly too low, their size-dependence nicely follows the experimental findings.

B. Nb₅ and Nb₅⁺

The experimental IR spectra of Nb₅ and Nb₅⁺ together with the calculated spectra of low energy isomers are shown in Fig. 2. For Nb₅ one identifies (at least) three distinct bands at 119, 189, and 262 cm^{-1} . The spectrum of the corresponding cation is more noisy and rather different with indications for two bands at 228 and 278 cm^{-1} . The seemingly “negative” absorptions in the spectrum of Nb₅⁺ and the positive signal above 370 cm^{-1} are related to small intensity drifts in the mass spectra that become amplified in the energy normalization of the IR spectrum due to the lower flux of IR radia-

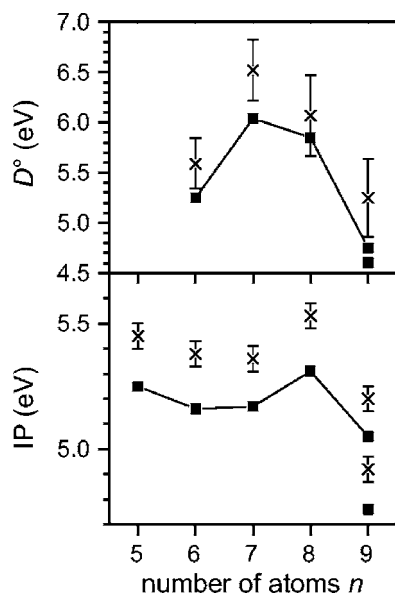


FIG. 1. Ionization potentials and dissociation energies of neutral niobium clusters. The calculated values for the structures identified in this study are represented by squares and the experimental values by crosses with error bars as given in the literature (Refs. 15 and 21). For Nb_9 , two isomers are present.

tion in that frequency range. Other clusters are, mainly because of their higher Ar complex abundances, much less affected.

Calculations find lowest energy isomers with similar geometries for the neutral species and the cation. The structure of 5^+A and $5A$ can be described as a trigonal bipyramid based on an obtuse isosceles. In the cation the basis of the isosceles is slightly elongated to 294 pm (289 pm in $5A$). All other bond lengths agree within 2 pm. For Nb_5^+ the triplet state isomer 5^+A is significantly lower in energy as compared to the singlet structure 5^+B by 0.16 eV. The positions of the two intense bands in the calculated spectrum of 5^+A agree well with the experimental findings. A minor contribution of 5^+B to the spectrum cannot be fully excluded due to some signal around 175 cm^{-1} . The calculated spectrum of $5A$ contains four bands in the range of the experiment and reproduces overall the experimental band pattern.

For the neutral clusters, geometries similar to $5A$ have been reported before as the ground state, mostly agreeing on a spin multiplicity of 2.^{39,40,42,44} Ionization has been found to lead only to minor structural changes under slight expansion.³⁹ Finally, the assigned structures of $5A$ and 5^+A perfectly match the 2B_1 and 3A_1 ground states of Nb_5 and Nb_5^+ , respectively, identified by Majumdar and Balasubramanian.^{43,44}

C. Nb_6 and Nb_6^+

For the neutral cluster, theory predicts two isoenergetic isomers, the dimer-capped rhombus $6B$ with C_2 symmetry that can also be described as a capped distorted trigonal bipyramid and the tetragonal-square bipyramid $6A$ (Fig. 3). Structure $6B$ has a singlet electronic state while $6A$ has two unpaired electrons. The spectroscopic signatures of $6A$ in the range of the experiment are two closely spaced peaks at 243

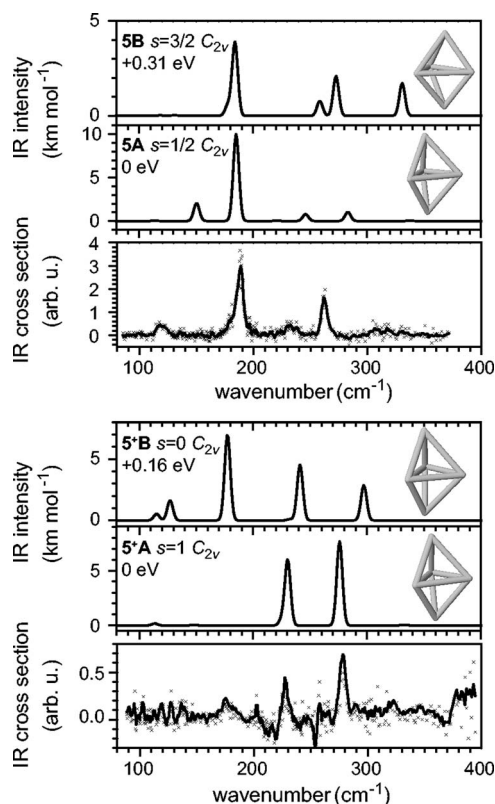


FIG. 2. Vibrational spectra of Nb_5 (upper panel) and Nb_5^+ (lower panel). The bottom traces in each panel show the experimental multiple photon dissociation spectra of the corresponding complexes with Ar atoms. They are compared with the calculated vibrational spectra for energetically low-lying isomers. The calculated stick spectra are folded with a Gaussian linewidth function of 5 cm^{-1} full width at half maximum for ease of comparison. The experimental data points are overlaid with a five-point running average to guide the eye.

and 259 cm^{-1} . The IR spectrum of $6B$ is more complex and fits the experiment best. Only the highest energy band is blueshifted in the calculated spectrum by 35 cm^{-1} . A minor contribution of $6A$ to the experimental spectrum cannot be fully excluded, since it shows peaks in the $230\text{--}260\text{ cm}^{-1}$ range, where both isomers have bands. Nevertheless, the bands around 190 cm^{-1} indicate that Nb_6 is predominantly present in the structure $6B$.

The cation seems to have a different geometry. Here again the spectrum of the energetically lowest isomer from the calculations 6^+A matches the experimental spectrum, although two of the three intense bands at 232, 258, and 285 cm^{-1} are not resolved in the experiment. The geometry of 6^+A is a tetragonal bipyramid (nonsquare, D_{2h} symmetry) with the lowest possible electronic spin $s=1/2$. The capped rhombus structure 6^+B is 0.12 eV higher in energy and shows a spectrum that does not comply with the experimental findings.

The neutral structure $6B$ corresponds to the “distorted prism” structure found before as the most stable isomer.⁴² It differs from the structures suggested in Refs. 39 and 40 by a rotation of the rhombus-capping dimer relative to the long rhombus diagonal by a dihedral angle of 18° .

The experimental vibrational spectrum of Nb_6^+ is remarkably similar to the spectrum of V_6^+ that is found to adopt a

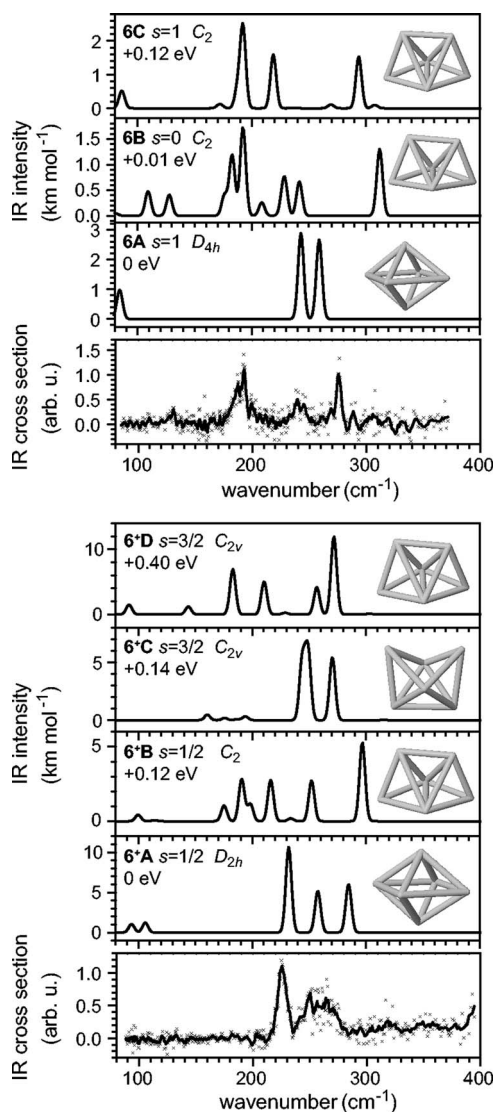


FIG. 3. Vibrational spectra of Nb_6 (upper panel) and Nb_6^+ (lower panel).

structure close to 6^+A ,¹⁰ the resonance frequencies in the spectrum of the Nb cluster appear to just be scaled down by a factor of about 0.9. This is less than if the vibrational frequencies would scale with the ratio of the reduced masses which can be approximated by $\sqrt{(m_V/m_{\text{Nb}})}$, i.e., 0.74. Apparently, the lowering of the vibrational frequencies due to the higher mass of Nb is partly counteracted by a stronger bonding in the niobium clusters. For comparison, an increased force constant is also found for the neutral niobium dimer.⁵⁷ This stronger bonding can be related to a more efficient overlap of the larger $4d$ orbitals of niobium than the $3d$ orbitals of vanadium.

D. Nb_7 and Nb_7^+

In case of the heptameric niobium clusters the experimental spectra are very similar for the cation and the neutral (Fig. 4). The spectra are dominated by two bands with their maxima at 213 and 271 cm^{-1} for the cation and at 223 and 274 cm^{-1} for the neutral cluster. The bands might contain unresolved structure as evidenced by the shoulders at 280 cm^{-1} (cation) and 212 cm^{-1} (neutral). Calculations find

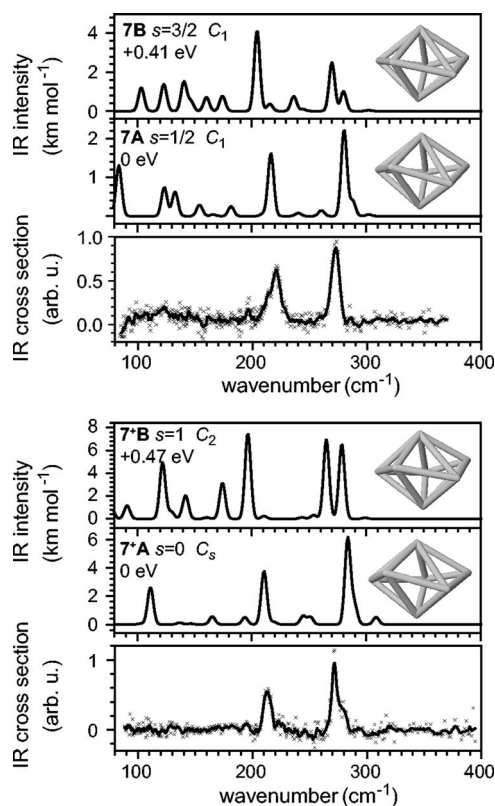


FIG. 4. Vibrational spectra of Nb_7 (upper panel) and Nb_7^+ (lower panel).

in both cases a distorted pentagonal bipyramid as the most stable isomer. The most intense bands are nicely reproduced by the calculations, for the cation even the shoulder at the high energy peak is found. The cationic structure 7^+A has C_s symmetry, and only one of the atoms of the pentagon is out of its plane. The neutral 7A is slightly more distorted. Such a structure is in agreement with earlier studies.^{39,40,42}

The similarities of the spectra of Nb_7^+ and Nb_7 to the spectrum of V_7^+ have been pointed out before.¹¹ As in the case of the hexamers, these similarities are related to a close resemblance in the geometric structures.

E. Nb_8 and Nb_8^+

The experimental and calculated spectra of the niobium octamers are shown in Fig. 5. Overall good agreement is found between the experimental spectra and those calculated for the lowest energy isomers 8^+A and 8A . Both have structures of a distorted bicapped octahedron, and have very similar geometries; only the distance between the capping atoms is in the neutral species about 5% longer than in the cation. The distorted hexagonal bipyramids 8^+B and 8B are in both cases significantly higher in energy and their spectra do not fit the experiments. Also, in earlier computational studies bicapped octahedra were found to be the most stable configurations for cation and neutral.^{41,42}

The Nb_8 cluster is one of the rare examples where vibrational data for a gas-phase metal cluster are available from earlier experiments.¹⁹ Vibrational frequencies for the anion and neutral have been obtained from a Franck-Condon analysis of the vibrational progressions found in the anion photoelectron spectrum. This results in frequencies of

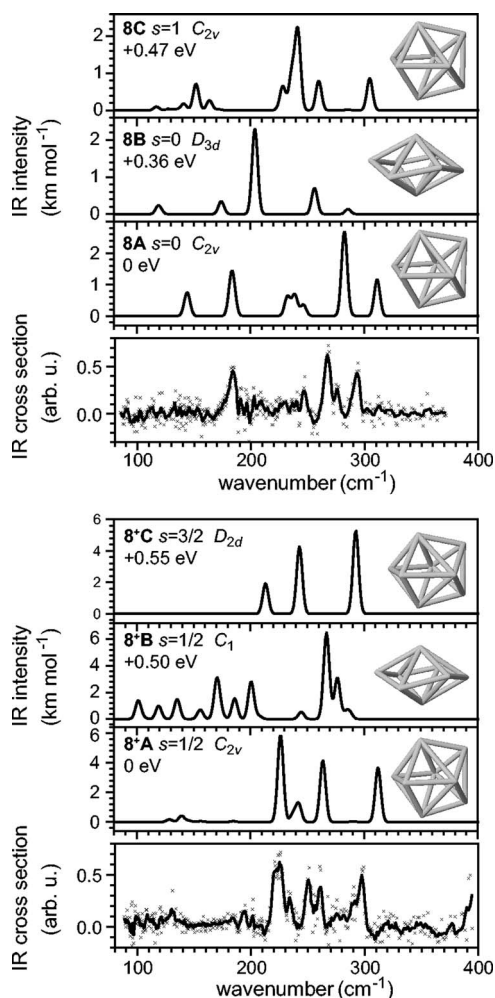


FIG. 5. Vibrational spectra of Nb_8 (upper panel) and Nb_8^+ (lower panel).

$180 \pm 15 \text{ cm}^{-1}$ for the neutral and $165 \pm 20 \text{ cm}^{-1}$ for the anion that are assigned to one of the totally symmetric A_1 modes of an isomer similar in structure to **8A**. The Franck-Condon analysis reveals that under electron detachment from the anion the structure is changed only very slightly. In fact, our study shows that neutral Nb_8 has practically the same geometry as suggested for the anion and this geometry is hardly changed in the cation. The reported frequency for neutral Nb_8 fits very well to our experimental far-IR spectrum that shows an intense peak at 184 cm^{-1} . In the calculated spectrum of **8A** we find in this range two closely spaced IR active vibrations at 186 and 188 cm^{-1} of A_1 and B_1 symmetries, respectively. The A_1 mode observed in the photoelectron spectrum is probably a fully delocalized stretching mode with out-of-phase stretching of the bonds perpendicular to the symmetry plane through the axial atoms of the octahedron. In other words, this mode can be described as an oblate/prolate transformation of the cluster.

F. Nb_9 and Nb_9^+

For the cationic cluster, a close resemblance is observed between experimental and theoretical spectra above 230 cm^{-1} for isomer **9A** (Fig. 6), indicating the predominance of this lowest energy isomer. This is different for the

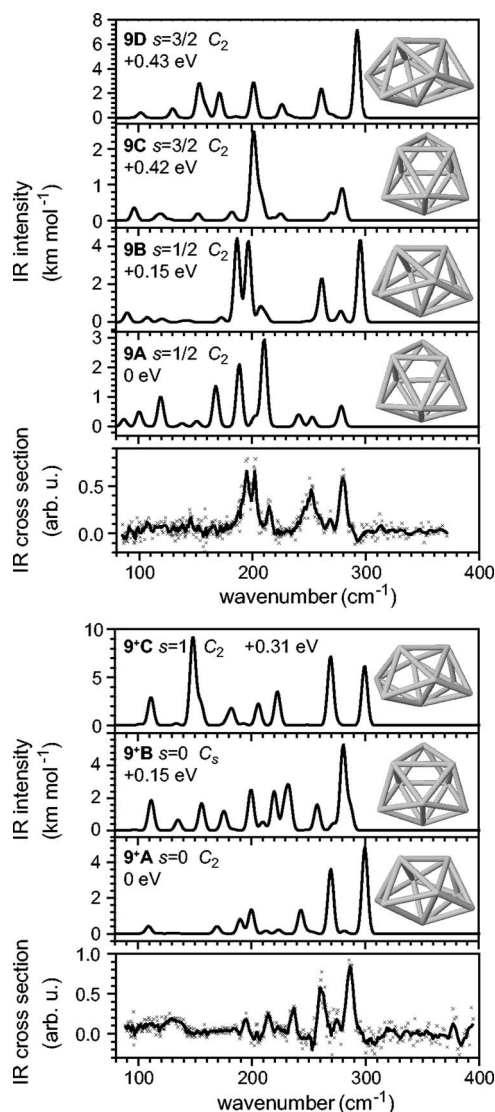


FIG. 6. Vibrational spectra of Nb_9 (upper panel) and Nb_9^+ (lower panel).

neutral cluster. Here the far-IR MPD spectrum of Nb_9Ar corresponds closely to the second isomer **9B**. Anyhow, Nb_9 is a special case: It is the only cluster where the far-IR-MPD spectra of the Nb_9Ar_m complexes change significantly with the number m of rare-gas atoms attached to the cluster. With increasing m some bands reduce in intensity, and others appear completely new. This is different to the behavior described in Sec. IV A, where with increasing m only a gradual increase in the band intensity is expected. We have discussed this in more detail in a previous Communication¹² and the dependence on m can be understood by the presence of two isomers with different affinity towards the argon atoms. The change in the spectra reflects the gradual change in the ratio of the isomer abundances with m and this has been used to obtain the isomer specific vibrational spectra.

Figure 6 shows the spectrum recorded via dissociation of the Nb_9Ar complex whose intensity is dominated by one of the isomers. The neutral Ar complexes are ionized with 6.42 eV photons, which efficiently ionizes both isomers. The near-threshold photoionization of the complex Nb_9Ar with 4.96 eV photons allows to selectively detect only a single

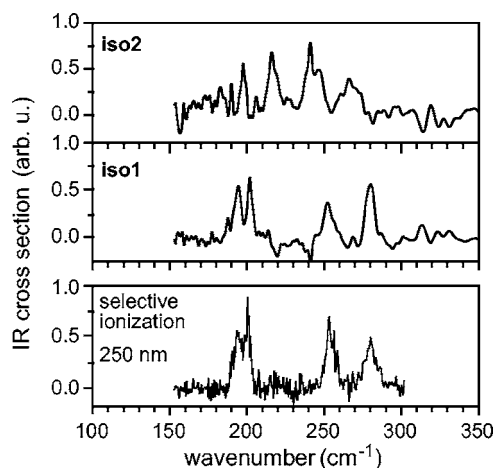


FIG. 7. Isomer selective IR spectra of Nb_9 . The two upper traces show the spectra extracted out of the spectra of Nb_9Ar_m ionized with an ArF laser (6.42 eV) using the procedures described in Ref. 12. The lower spectrum is measured with selective ionization of the Ar complex of a single isomer with 250 nm radiation (4.96 eV).

isomer. Its IR spectrum is shown in Fig. 7 together with the isomer specific spectra that are extracted from the spectra of Nb_9Ar_m ($m=1-4$). Details of the extraction procedure have been reported before in Ref. 12 and only the results are discussed here. The spectrum of the isomer with the lower ionization potential ionized with the 4.96 eV photons closely resembles the spectrum of the isomer with the lower affinity towards Ar (iso1) and fits the spectrum of 9B. Its structure is similar to the structure 9⁺A found for the cation, a buckled hexagon capped on one side by a dimer and on the other side by a single atom.

The calculated ground state of Nb_9 is 9A, a distorted triply capped trigonal prism. The agreement of its spectrum with that of the second isomer iso2 is not very clear, although there is resemblance in the band positions, but the intensities do not match. The experimental spectrum can be affected by the multiple photon absorption process, or the interaction with multiple Ar atoms might affect the structure of this isomer, even though such a strong effect is not observed for any other niobium cluster. An additional evidence for the structural assignment is obtained from the calculated adiabatic ionization potentials of the Nb_9 isomers. We find values of 5.05 and 4.76 eV that correspond reasonably well to the experimental values of 5.20 and 4.92 eV.^{14,15}

The monomer/dimer-capped hexagon and the triply capped trigonal prism have been identified before as low-lying isomers of Nb_9 and Nb_9^+ in DFT studies. Their energetic ordering is found to depend on the employed functional, i.e., using LSDA one identifies for the neutral a structure such as 9B as more stable, whereas the order is reversed by using the Becke-Lee-Yang-Parr (BLYP) (Ref. 41) or a GGA functional.⁴² For the cation BLYP and LSDA consistently favor the capped hexagon.⁴¹

V. CONCLUSIONS

Multiple photon dissociation spectroscopy on the Ar complexes of neutral and cationic niobium clusters is used to obtain their vibrational spectra in the far-infrared. Although, this method actually probes the vibrational structure of the

Ar complexes, a close resemblance is found with the linear absorption spectra of the bare metal clusters, calculated by means of the density-functional theory. For most of these clusters a best agreement between experimental and calculated spectra is obtained for the lowest energy isomers. This finding indicates that the binding of the Ar does not significantly affect the internal geometric or electronic structures of the investigated niobium clusters.

All clusters in the investigated size range form compact three-dimensional structures such as distorted bipyramids, but there is not yet a common buildup principle for the cluster geometries. Although the experimental vibrational spectra are, except for $\text{Nb}_7^{0/+}$, rather different for neutral and cationic clusters, the comparison with theory reveals that the geometric structures, with the exception of $\text{Nb}_6^{0/+}$, do hardly change upon removal of an electron.

Strong similarities are found between the spectra of Nb_6^+ , Nb_7^+ , and Nb_7 and the spectra of the corresponding vanadium cluster cations. Although there are not that obvious correlations in the spectra for the other sizes, for most niobium clusters the identified geometric structures are very similar to those of the cationic vanadium clusters except for Nb_6 and Nb_9^+ .

The comparison of the experimental spectra with the present and earlier theoretical studies shows that the density-functional theory applying the generalized gradient approximation is well suited to describe these small niobium clusters and is (in most cases) capable of predicting the correct ground state structures. However, even if there exists a reliable method of calculating the electronic structure, the chance for identifying the correct ground state is limited by the method for scanning the configurational space. For larger clusters, therefore, one can anticipate a substantial benefit from the combination of DFT with global optimization methods.

ACKNOWLEDGMENTS

We gratefully acknowledge the support by the "Stichting voor Fundamenteel Onderzoek der Materie" (FOM) in providing the required beam time on FELIX and highly appreciate the skillful assistance by the FELIX staff, in particular, Dr. B. Redlich and Dr. A.F.G. van der Meer. We thank Accelrys for providing the DMOL³ software to the California NanoSystems Institute. We acknowledge helpful suggestions by the referee.

¹S. J. L. Billinge and I. Levin, *Science* **316**, 561 (2007).

²A. A. Shvartsburg, R. R. Hudgins, P. Dugourd, and M. F. Jarrold, *Chem. Soc. Rev.* **30**, 26 (2001).

³P. Weis, *Int. J. Mass. Spectrom.* **245**, 1 (2005).

⁴X. Xing, B. Yoon, U. Landman, and J. H. Parks, *Phys. Rev. B* **74**, 165423 (2006).

⁵M. N. Blom, D. Schooss, J. Stairs, and M. M. Kappes, *J. Chem. Phys.* **124**, 244308 (2006).

⁶S. Bulusu, X. Li, L.-S. Wang, and X. C. Zeng, *Proc. Natl. Acad. Sci. U.S.A.* **103**, 8326 (2006).

⁷O. Kostko, B. Huber, M. Moseler, and B. von Issendorff, *Phys. Rev. Lett.* **98**, 043401 (2007).

⁸K. R. Asmis, A. Fielicke, G. von Helden, and G. Meijer, in *Atomic Clusters: From Gas Phase to Deposited*, The Chemical Physics of Solid Surfaces Vol. 12, edited by D. P. Woodruff (Elsevier, Amsterdam, 2007) pp. 327–375.

- ⁹ A. Fielicke, A. Kirilyuk, C. Ratsch, J. Behler, M. Scheffler, G. von Helden, and G. Meijer, *Phys. Rev. Lett.* **93**, 023401 (2004).
- ¹⁰ C. Ratsch, A. Fielicke, A. Kirilyuk, J. Behler, G. von Helden, G. Meijer, and M. Scheffler, *J. Chem. Phys.* **122**, 124302 (2005).
- ¹¹ A. Fielicke, G. von Helden, and G. Meijer, *Eur. Phys. J. D* **34**, 83 (2005).
- ¹² A. Fielicke, C. Ratsch, G. von Helden, and G. Meijer, *J. Chem. Phys.* **122**, 091105 (2005).
- ¹³ R. L. Whetten, M. R. Zakin, D. M. Cox, D. J. Trevor, and A. Kaldor, *J. Chem. Phys.* **85**, 1697 (1986).
- ¹⁴ M. B. Knickelbein and S. Yang, *J. Chem. Phys.* **93**, 1476 (1990).
- ¹⁵ M. B. Knickelbein and S. Yang, *J. Chem. Phys.* **93**, 5760 (1990).
- ¹⁶ B. A. Collings, A. H. Amrein, D. M. Rayner, and P. A. Hackett, *J. Chem. Phys.* **99**, 4174 (1993).
- ¹⁷ H. Kietzmann, J. Morenzin, P. S. Bechthold, G. Ganteför, W. Eberhardt, D.-S. Yang, P. A. Hackett, R. Fournier, T. Pang, and C. Chen, *Phys. Rev. Lett.* **77**, 4528 (1996).
- ¹⁸ H. Kietzmann, J. Morenzin, P. S. Bechthold, G. Ganteför, and W. Eberhardt, *J. Chem. Phys.* **109**, 2275 (1998).
- ¹⁹ T. P. Marcy and D. G. Leopold, *Int. J. Mass. Spectrom.* **196**, 653 (2000).
- ²⁰ G. Wrigge, M. A. Hoffmann, B. von Issendorff, and H. Haberland, *Eur. Phys. J. D* **24**, 23 (2003).
- ²¹ D. A. Hales, L. Lian, and P. B. Armentrout, *Int. J. Mass Spectrom. Ion Process.* **102**, 269 (1990).
- ²² S. K. Loh, L. Lian, and P. B. Armentrout, *J. Am. Chem. Soc.* **111**, 3167 (1989).
- ²³ M. B. Knickelbein and W. J. C. Menezes, *Phys. Rev. Lett.* **69**, 1046 (1992).
- ²⁴ W. J. C. Menezes and M. B. Knickelbein, *J. Chem. Phys.* **98**, 1856 (1993).
- ²⁵ B. A. Collings, K. Athanassenas, D. M. Rayner, and P. A. Hackett, *Z. Phys. D: At., Mol. Clusters* **26**, 36 (1993).
- ²⁶ M. R. Zakin, D. M. Cox, and A. Kaldor, *J. Phys. Chem.* **91**, 5224 (1987).
- ²⁷ C. Berg, M. Beyer, U. Achatz, S. Joos, G. Niedner-Schatteburg, and V. E. Bondybey, *J. Chem. Phys.* **108**, 5398 (1998).
- ²⁸ A. B. Vakhtin and K. Sugawara, *J. Chem. Phys.* **115**, 3629 (2001).
- ²⁹ J. M. Parnis, E. Escobar-Cabrera, M. G. K. Thompson, J. P. Jacula, R. D. Laffleur, A. Guevara-García, A. Martínez, and D. M. Rayner, *J. Phys. Chem. A* **109**, 7046 (2005).
- ³⁰ J. L. Elkind, F. D. Weiss, J. M. Alford, R. T. Laaksonen, and R. E. Smalley, *J. Chem. Phys.* **88**, 5215 (1988).
- ³¹ M. R. Zakin, R. O. Brickman, D. M. Cox, and A. Kaldor, *J. Chem. Phys.* **88**, 3555 (1988).
- ³² Y. Hamrick, S. Taylor, G. W. Lemire, Z.-W. Fu, J.-C. Shui, and M. D. Morse, *J. Chem. Phys.* **88**, 4095 (1988).
- ³³ Y. M. Hamrick and M. D. Morse, *J. Phys. Chem.* **93**, 6494 (1989).
- ³⁴ A. Bérces, P. A. Hackett, L. Lian, S. A. Mitchell, and D. M. Rayner, *J. Chem. Phys.* **108**, 5476 (1998).
- ³⁵ C. Berg, T. Schindler, M. Kantlehner, G. Niedner-Schatteburg, and V. E. Bondybey, *Chem. Phys.* **262**, 143 (2000).
- ³⁶ M. B. Knickelbein, *J. Chem. Phys.* **118**, 6230 (2003).
- ³⁷ R. Moro, X. Xu, S. Yin, and W. A. de Heer, *Science* **300**, 1265 (2003).
- ³⁸ X. Xu, S. Yin, R. Moro, A. Liang, J. Bowlan, and W. A. de Heer, *Phys. Rev. B* **75**, 085429 (2007).
- ³⁹ L. Goodwin and D. R. Salahub, *Phys. Rev. A* **47**, R774 (1993).
- ⁴⁰ H. Grönbeck and A. Rosén, *Phys. Rev. B* **54**, 1549 (1996).
- ⁴¹ H. Grönbeck, A. Rosén, and W. Andreoni, *Phys. Rev. A* **58**, 4630 (1998).
- ⁴² V. Kumar and Y. Kawazoe, *Phys. Rev. B* **65**, 125403 (2002).
- ⁴³ D. Majumdar and K. Balasubramanian, *J. Chem. Phys.* **115**, 885 (2001).
- ⁴⁴ D. Majumdar and K. Balasubramanian, *J. Chem. Phys.* **121**, 4014 (2004).
- ⁴⁵ D. Majumdar and K. Balasubramanian, *J. Chem. Phys.* **119**, 12866 (2003).
- ⁴⁶ J. Zhao, X. Chen, and G. Wang, *Phys. Lett. A* **214**, 211 (1996).
- ⁴⁷ S. K. Nayak, B. K. Rao, S. N. Khanna, and P. Jena, *Chem. Phys. Lett.* **259**, 588 (1996).
- ⁴⁸ R. Fournier, T. Pang, and C. Chen, *Phys. Rev. A* **57**, 3683 (1998).
- ⁴⁹ J. E. Fowler, A. García, and J. M. Ugalde, *Phys. Rev. A* **60**, 3058 (1999).
- ⁵⁰ K. E. Andersen, V. Kumar, Y. Kawazoe, and W. E. Pickett, *Phys. Rev. Lett.* **93**, 246105 (2004).
- ⁵¹ C. M. Chang and M. Y. Chou, *Phys. Rev. Lett.* **93**, 133401 (2004).
- ⁵² W. Fa, C. Luo, and J. Dong, *Phys. Rev. B* **71**, 245415 (2005).
- ⁵³ T. R. Walsh, *J. Chem. Phys.* **124**, 204317 (2006).
- ⁵⁴ L. L. Wang and D. D. Johnson, *Phys. Rev. B* **75**, 235405 (2007).
- ⁵⁵ Z. Hu, B. Shen, Q. Zhou, S. Deosaran, J. R. Lombardi, and D. M. Lindsay, *Proc. SPIE* **1599**, 65 (1992).
- ⁵⁶ M. Moskovits and W. Limm, *Ultramicroscopy* **20**, 83 (1986).
- ⁵⁷ A. M. James, P. Kowalczyk, R. Fournier, and B. Simard, *J. Chem. Phys.* **99**, 8504 (1993).
- ⁵⁸ H. Wang, R. Craig, H. Haouari, Y. Liu, J. R. Lombardi, and D. M. Lindsay, *J. Chem. Phys.* **105**, 5355 (1996).
- ⁵⁹ D. Oepts, A. F. G. van der Meer, and P. W. van Amersfoort, *Infrared Phys. Technol.* **36**, 297 (1995).
- ⁶⁰ B. Delley, *J. Chem. Phys.* **92**, 508 (1990).
- ⁶¹ J. P. Perdew, K. Burke, and M. Ernzerhof, *Phys. Rev. Lett.* **77**, 3865 (1996).
- ⁶² J. Oomens, A. G. G. M. Tielens, B. Sartakov, G. von Helden, and G. Meijer, *Astrophys. J.* **591**, 968 (2003).
- ⁶³ Y. Nakagawa and A. D. B. Woods, *Phys. Rev. Lett.* **11**, 271 (1963).
- ⁶⁴ R. I. Sharp, *J. Phys. C* **2**, 421 (1969).
- ⁶⁵ R. Moro, S. Yin, X. Xu, and W. A. de Heer, *Phys. Rev. Lett.* **93**, 086803 (2004).